

OMAE2011-498-)

EFFECTS OF VARYING TENSION AND STIFFNESS ON DYNAMIC CHARACTERISTICS AND VIV OF SLENDER RISER

Chen Weimin

Key Laboratory of Environmental
Mechanics, Institute of
Mechanics, CAS
Beijing 100190, China

Zheng Zhongqin

Key Laboratory of Environmental
Mechanics, Institute of
Mechanics, CAS
Beijing 100190, China

Li Min

School of Aeronautics Sciences
and Engineering, Beijing
University of Aeronautics and
Astronautics
Beijing 100191, China

ABSTRACT

A time-domain approach for predicting dynamic characteristics and vortex-induced vibration (VIV) response of deepwater risers is proposed by coupling finite element simulation and a hydrodynamic model. Numerical results indicate that axially varying structural parameters can efficiently change the modal wave length as well as the modal displacement. Further, VIV response indicates that vibration amplitude depends on a complex synthetical effect of tension, stiffness and wave length. Generally speaking, for lower modes the response amplitude is larger at the axial position where tension is smaller, whereas for higher modes the response amplitude is larger at the axial position where bending stiffness is lower. Moreover, vibration wave velocity increases with increasing modal wave length.

KEYWORDS: deepwater riser; varying tension; vortex-induced vibration; dynamic characteristics

1. INTRODUCTION

As the oil exploitation extending to deepwater ocean, the length of riser gets larger and the structural configuration becomes more complex, e.g. the outer or inner diameter gradually varies along the length of riser rather than a constant value. Additionally, the axial tension is no longer considered as constant along the overall length of riser due to considerable structure weight. Therefore, the dynamic analysis such as the dynamic characteristics and VIV of slender riser with varying structural properties becomes a new challenging problem^[1-3].

In this study, a model of dynamic characteristics and VIV by means of finite element simulation combined with a hydrodynamic model taking account of the interaction between fluid and structure, i.e. a coupling analysis approach in time-domain for deepwater risers, is proposed. Generally, the hydrodynamic force such as vortex-induced lift depends on the ambient fluid dynamics and structure motion, so is expressed as a function of variables related to both fluid and structure.

However, in existing model for dynamic response an iterative calculation is needed^[4-7] because the vibration amplitude of structure is unknown before the calculation. Here, an alternative lift model described by the instantaneous motion of structure is proposed so as to avoid costly iterations, and be efficient enough for time domain analysis of finite element code.

The dynamic characteristics of riser with axially varying structural properties are examined by numerical simulations. It is observed that the modal wave length and displacements are sensitive to the varying structural properties. Further, numerical results of VIV indicate that the vibration amplitude depends on a complex synthetical influence of tension, stiffness and modal wave length.

2. NUMERICAL MODELING

2.1 Hydrodynamic Model and Finite Element Simulation

The dynamic equilibrium equation of a tension Euler beam is as follow:

$$m \frac{\partial^2 y}{\partial t^2} + c \frac{\partial y}{\partial t} + \frac{\partial^2}{\partial x^2} [EI(x) \frac{\partial^2 y}{\partial x^2}] - \frac{\partial}{\partial x} [T(x) \frac{\partial y}{\partial x}] = f(x, t) \quad (1)$$

where m and c are the structural mass and damping of unit length respectively, $EI(x)$ and $T(x)$ are the bending stiffness and axis tension, $y(x, t)$ is the cylinder motion. $f(x, t)$ is the hydrodynamic force consisting of vortex-induced lift force $f_v(x, t)$ and motion-induced fluid damping force $f_f(x, t)$, which are given respectively as follows:

$$f_v(x, t) = (1/2)C_L \rho V^2 D \sin \omega_v t \quad (2a)$$

$$f_f(z, t) = \frac{1}{2}C_D \rho D(V - \dot{y})|V - \dot{y}| + C_A \frac{1}{4}\pi D^2 \rho (\dot{V} - \ddot{y}) + \frac{1}{4}\pi D^2 \rho \dot{V} \quad (2b)$$

where C_L is the vortex-induced lift coefficient, ρ and V are the density and velocity of fluid respectively, ω_v is the vortex shedding frequency. C_D and C_A are the drag and added mass coefficient respectively, which can be determined by experiments.

Generally, C_L is expressed as a function related to variables describing structure motion so as to take account of the interaction between fluid dynamic and structural dynamic. Existing lift model is presented as a hyperbolic curve of C_L against structural motion

amplitude (see Fig.1), of which the coefficients such as $C_{L,max}$ and $C_{L,A/D=0}$ are based on experimental results. However, for our problem the motion amplitude is unknown before the calculation. An iterative calculation is used in previous methods, which is computationally expensive and is unfortunately not suitable to the time domain calculation of dynamic response simulated by FEM (finite element method) codes. Here, an alternative lift curve describing by the instantaneous motion of structure is proposed.

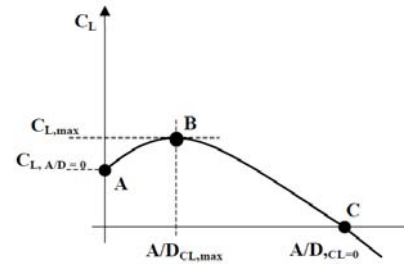


Figure 1 Lift curve

The presented lift coefficient C_L as a function of structural velocity is assumed to be capable of inputting the same work to the structure in a motion period as the previous one is. And C_L is assumed be:

$$C_L(\dot{y}) = C_{L0} + a\dot{y} + b\dot{y}^2 + c\dot{y}^3 \quad (3)$$

The structural motion in lock-in is assumed as $y = A \sin(\omega t)$. Then the works done by a constant lift force $F_0 = (1/2)2C_{L0}\rho V^2 D$ and an unsteady lift force having a form of

$$F = F_0 \cos(\omega t) + a\dot{y} + b\dot{y}^2 + c\dot{y}^3 \quad (4)$$

in a one-fourth period can be respectively written as:

$$W_0 = \int_0^T F_0 A \omega (\cos \omega t)^2 dt = \frac{\pi}{4} F_0 A \quad (5a)$$

$$W_1 = \int_0^T F A \omega (\cos \omega t)^2 dt \quad (5b)$$

$$= \frac{\pi}{4} F_0 A + a' A^2 + b' A^3 + c' A^4$$

$$\text{Or } W_1/W_0 = 1 + a'' A + b'' A^2 + c'' A^3 \quad (6)$$

$$\text{where } a'' = \frac{\omega}{F_0} a, \quad b'' = \frac{8\omega^2}{3\pi F_0} b \quad \text{and} \quad c'' = \frac{3\omega^3}{4F_0} c.$$

Therefore a new lift coefficient can be got as

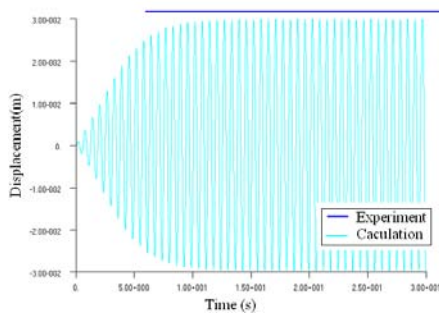
$$C_L'' = C_{L0}(1 + a'' A + b'' A^2 + c'' A^3) \quad (7)$$

The values of a , b , c and C_{L0} can be resolved by making the new curve fit with the original one at some key points such as points A, B and C in Fig.1.

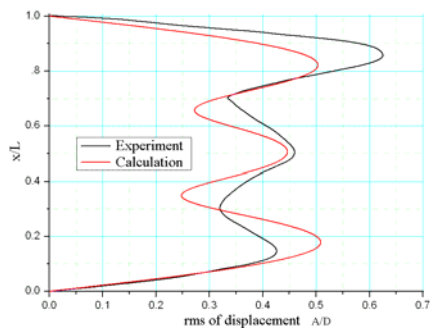
2.2 Validation against Experimental Results

Based on the lift model presented above, finite element simulations are carried out to calculate the dynamic response of a riser undergoing VIV. To validate the proposed finite element model, the numerical results are compared to experimental results (see Fig. 3), i.e. a rigid cylinder in uniform current by Williamson(1999)^[8], a flexible cylinder in stepped by Chaplin(2005)^[9] and sheared currents by Trim(2005)^[10].

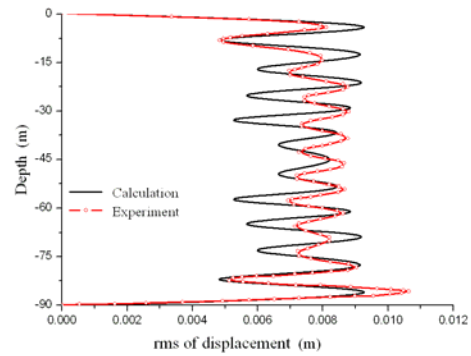
In our numerical simulation, the hydrodynamic coefficients are $C_A = 1.0$, $C_d = 1.2$; and the lift coefficients are $C_L = 0.5 + 1.82A - 1.29A^2 - 0.707A^3$ and $C_L = 0.22 + 1.62A - 2.31A^2 + 0.754A^3$ for rigid and flexible cylinder respectively. Figure 3 indicates that the calculated amplitude agree with experimental results for both rigid and flexible cylinder in various flow.



(a) Rigid cylinder in uniform flow



(b) Flexible cylinder in stepped flow



(c) Flexible cylinder in sheared flow

Figure 3 Comparisons of VIV response between the presented numerical simulation and the existing experimental results of (a) rigid cylinder in uniform flow; (b) flexible cylinder in stepped flow; and (c) flexible cylinder in sheared flow.

3. NUMERICAL RESULTS AND DISCUSSIONS

3.1 Effect of Varying Tension on Dynamic Characteristics

The riser (shown in Fig.4) is 1000m long and the outer and inner diameters are 0.500m and 0.445m respectively. The top tension T is 6.24×10^6 N (at the right end of the riser) and the top tension factor T/W is 1.57 (W is the riser weight). The tension along the overall riser length decreases linearly from the right end to the left end of the riser due to the effect of the riser weight W (along the opposite direction of axis x).

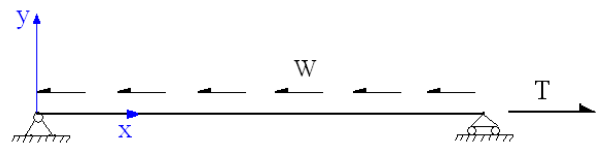


Figure 4 Sketch of the riser with varying tension

The natural frequencies of the riser with varying tension are presented and compared with that of riser with constant tension (by neglecting the effect of structural weight) in Fig.5. The selected mode shapes are presented in Fig. 6. These two figures indicate that: 1) the frequency decreases due to the decrease of overall tension along the riser length; 2) the wave length becomes longer in regions of higher tension along the riser length; 3) the peak of the amplitude moves from regions of lower tension to regions of higher tension as the mode number increases. The theoretical explanations about these phenomena will be given later.

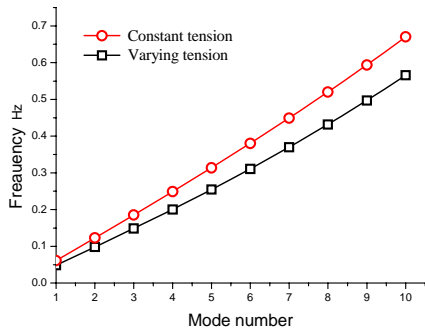


Figure 5 Natural frequencies of riser respectively with varying and constant tension

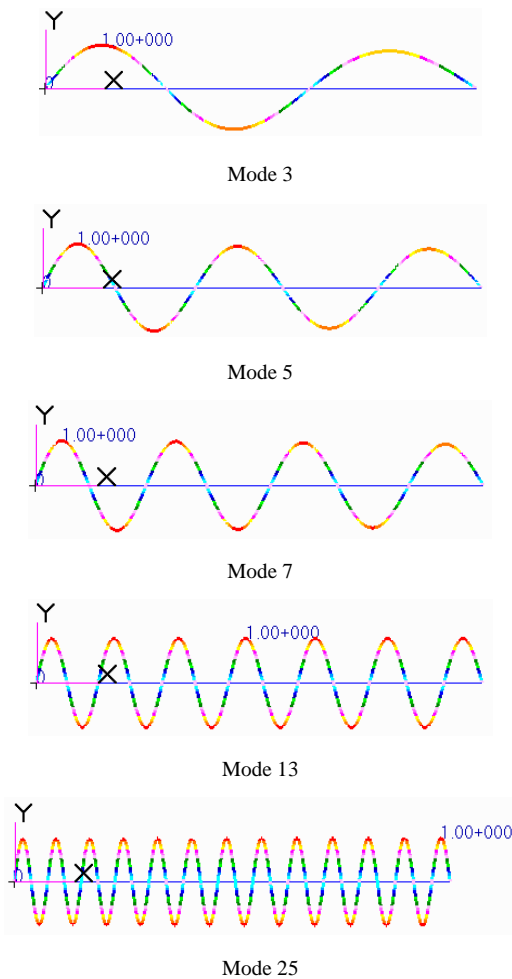


Figure 6 Modal shape of riser with varying tension dropping from right to left.

3.2 Effect of Varying Stiffness on Dynamic Characteristics

In practice, especially for case of deepwater, the wall thickness of riser typically changes along the length because of material and structural efficiency. Here, the variation of bending stiffness $EI(x)$ is considered by varying wall thickness. The riser is divided into five parts with the same outer diameter but different inner

diameters: 0.365 m, 0.385 m, 0.405 m, 0.425 m and 0.445 m. So the stiffness is higher at the bottom of the riser. Gravity is neglected, or the tension is constant, 6.24×10^6 N, along the riser length.

Selected mode shapes are presented in Fig. 7. It shows that: 1) both wave length and amplitude increase with the decrease of stiffness; 2) the amplitude decreases due to the increase of stiffness, or its distribution along the riser length is inversely proportional to the stiffness distribution especially for higher mode, e.g. mode 43.

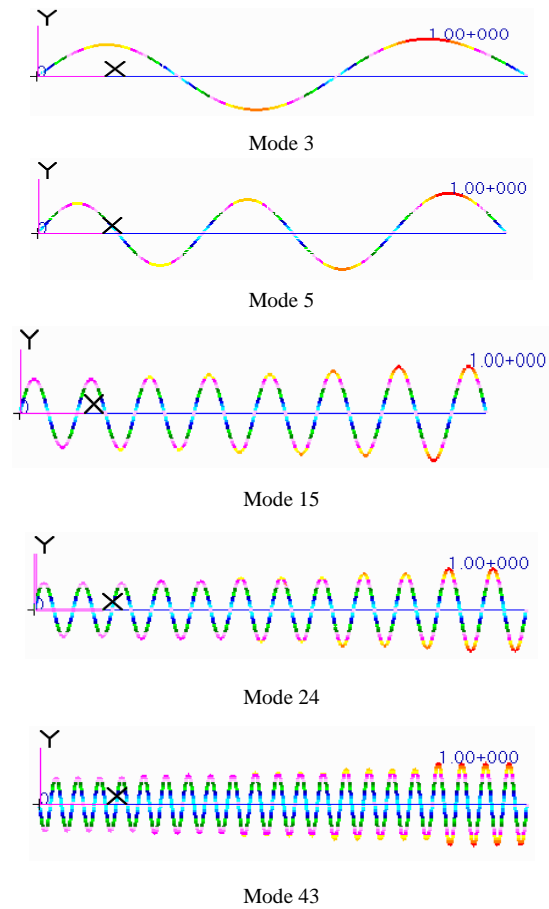


Figure 7 Modal shape of riser with varying stiffness increasing from right to left.

3.3 Theoretical Analysis

For a tension beam written as Eq. (1), if its solution is assumed as $y = \bar{y}(x)e^{-i\omega t}$ and the right side is set to be, the governing equation can be written as

$$EI(x) \frac{d^4 \bar{y}}{dx^4} + \frac{d(EI)}{dx} \frac{d^3 \bar{y}}{dx^3} + \frac{d^2(EI)}{dx^2} \frac{d^2 \bar{y}}{dx^2} - T \frac{d^2 \bar{y}}{dx^2} - \frac{dT}{dx} \frac{d\bar{y}}{dx} - m\omega^2 \bar{y} - ic(x)\omega \bar{y} = 0 \quad (8)$$

By WKB method^[3], we let

$$\bar{y}(x) = e^{i\theta(x)} \{a_0(x) + a_1(x) + a_2(x)\} \quad (9)$$

where a_1 and a_2 are higher order corrections. Also, we let

$$d\theta(x)/dx = \gamma(x) \quad (10)$$

where $\gamma(x)$ is local wave number. Substituting Eq.s (9) and (10) into Eq. (8) and remaining the leading order terms yields the dispersion relation as follow:

$$EI(x)\gamma^4(x) + T(x)\gamma^2(x) - m(x)\omega^2 - ic(x) + k(x) = 0 \quad (11)$$

Remaining the next order terms yields:

$$EI(-6i\gamma'\gamma^2 a_0 + \gamma^4 a_1 - 4i\gamma^3 a_0') + 2(EI)'(-i\gamma^3 a_0) - T(i\gamma a_0 - \gamma^2 a_1 + 2i\gamma a_0') - T'(i\gamma a_0) - m\omega^2 a_1 - ic\omega a_1 = 0 \quad (12)$$

Eliminating all terms with a_1 by means of Eq. (11) yields that the amplitude $a_0(x)$ along the riser axis would obey

$$a_0^2(x)[EI(x)\gamma^3(x) + (1/2)T(x)\gamma(x)] = cons. \quad (13)$$

For case of beam with varying tension, $\gamma(x)$ would become smaller or wave length $\lambda(x)$ ($\lambda(x) = 2\pi/\gamma(x)$) would become larger with increasing tension $T(x)$. That is as shown in Fig.6. The value of amplitude $a_0(x)$ depends on the value of the terms in square bracket of Eq. (13). For modal shape of lower mode, the second term in the square bracket, $(1/2)T(x)\gamma(x)$, dominates its value due to stronger effect of tension. So at position x with larger tension $T(x)$, the value of the square bracket is larger, and then the amplitude $a_0(x)$ would be smaller because of their product being a constant required by Eq. (13). However, for higher modes, the first term in the square bracket, $EI(x)\gamma^3(x)$, dominates the total value due to stronger effect of bending stiffness. So at position x with larger tension $T(x)$ (or smaller $\gamma(x)$), the value of the square bracket is smaller because of the drop of $EI(x)\gamma^3(x)$. Therefore, the amplitude $a_0(x)$ would be larger as required by Eq. (13). The moving peak of amplitude with increasing mode number is shown in Fig.6.

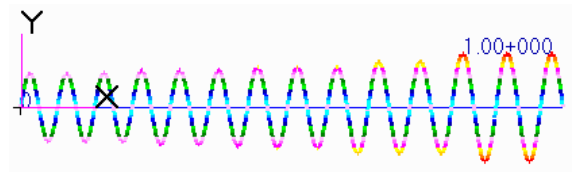
Similarly, for case of beam with varying $EI(x)$, amplitude peak would move from the axial position with larger stiffness $EI(x)$ to the position with smaller $EI(x)$ as the mode number increasing (see Fig.7).

3.4 VIV of Riser with Varying Structural Properties

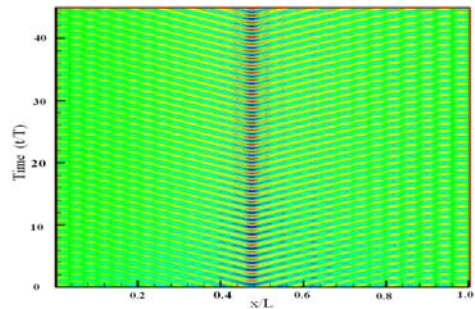
The parameters of the model are same with those in section 3.2. Also the gravity is taken into account. Two cases of top tensions $T = 1.91 \times 10^7$ N and $T = 6.24 \times 10^6$ N are examined. In practice, the motion of top end induced by environmental wave and current can introduce pronounced influence on the submarine structure^[11-13]. For example, the vertical motion (heave) of the platform may make the riser tension change remarkably, or even, in extreme case, into negative value at certain positions.

The hydrodynamic forces described above are loaded on the riser. The vortex-induced lift $f_v(x,t)$ is loaded at the centers of modal shape, and the fluid damping force $f_f(x,t)$ is uniformly distributed along the riser. The frequency of the lift is consistent with the natural frequency of the riser ranging from mode 1-35. VIV response is calculated numerically by the FEM model presented in this paper.

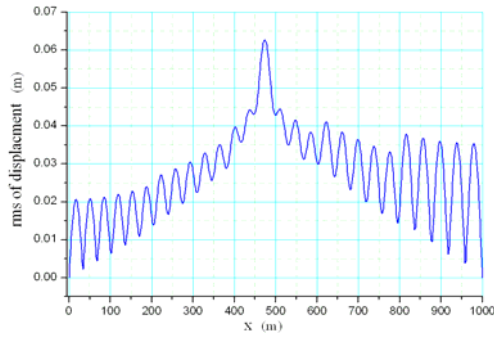
For case of higher tension, $T = 1.91 \times 10^7$ N, selected results of mode 27 are presented in Fig.8 where the vortex-induced lift force acts at the seventh trough from the left end, i.e. $x/L = 0.47$. The mode shape is plotted in Fig.8a. The temporal-spatial evolution and rms of displacement are plotted in Fig.8b and Fig.8c respectively.



a. Mode shape of mode 27



b. Temporal-spatial evolution of VIV displacement



c. Rms of displacement

Figure 8 Mode shape and VIV response of riser with axially varying structural properties. (mode 27, tension $T = 1.91 \times 10^7$ N.)

The results of displacement response (see Fig.8 b and c) indicate that the vibration propagates from the excitation point to the ends of the riser in a manner of intermediate wave^[14,15], i.e. between a standing and travelling wave. The displacement attenuates slowly at the right part of the riser and quickly at the left part due to the increase of bending stiffness from the right to left. In fact, the value of displacement depends on both attenuation velocity and propagation distance. Additionally, the wave velocity becomes fast with increasing wave length.

For case of lower tension $T = 6.24 \times 10^6$ N less than structural weight, the mode shapes for selected modes, i.e. mode 3, 5, 6, 7, 9, 11 and 29, are presented in Fig.9. It shows that a sinusoidal approximation is only appropriate for higher modes (higher than mode 7). For lower modes there is no displacement in regions of higher tension.

Among the VIV results, the abrupt displacement augmentation at the position with negative tension observed (as shown in Fig.10). The maximum augmentation is around 10~20 times, which can introduce instability and consequent damage of structure. Thus, this dangerous case should be avoided in practical engineering.

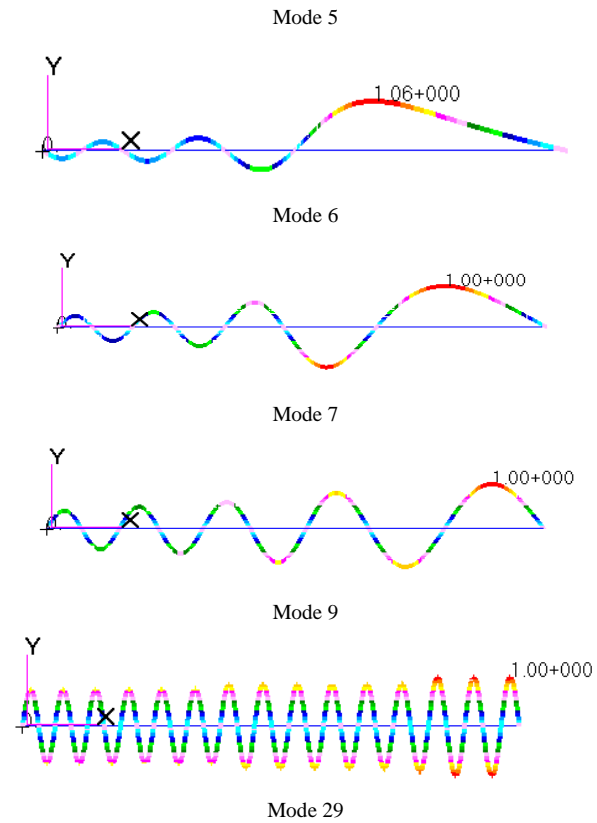
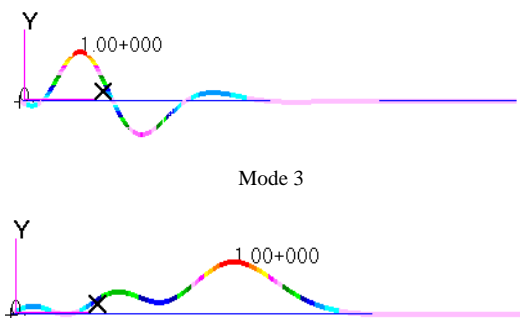


Figure 9 Selected modal shapes of riser with varying stiffness for case of lower tension $T = 6.24 \times 10^6$ N.

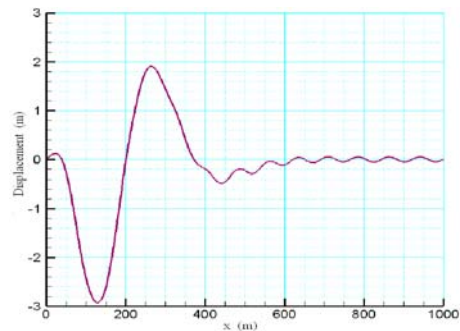


Figure 10 VIV response of riser with varying stiffness for case of lower tension $T = 6.24 \times 10^6$ N.

4. CONCLUSIONS

A prediction approach for predicting dynamic characteristics and VIV of deepwater riser, using finite element simulation combined with a coupling hydrodynamic model in time domain, is proposed. Satisfied agreements of displacement prediction with experiments are observed, though the presented approach based on an empirical lift curve still can not fully capture the physics of VIV such as wake-jumping and hysteresis. Effects of axially varying structural properties are examined. Based on our numerical results, we draw following conclusions:

1) Along the riser length, modal wave length increases with increasing tension or decreasing bending stiffness.

2) Modal amplitude is influenced by varying tension, stiffness and wave number (or wave length) as required by Eq.(13). Generally, for lower modes the amplitude gets larger at the axis position where tension is smaller, whereas for higher modes the amplitude gets larger at the axis position where bending stiffness is lower.

3) For VIV response, vibration wave velocity would increase, i.e. the vibration would propagate fast along the riser, due to the increasing modal wave length.

4) The displacement augmentation, around 10~20 times, at the position with lower tension can introduce instability and consequent damage of structure. It should be paid attention in practical engineering.

- [9] Chaplin J.R., P.W. Bearman, F.J. Huera et al. 2005, Laboratory measurements of vortex-induced vibrations of a vertical tension riser in a stepped current. *Journal of Fluids and Structures*, 21, pp:3–24.
- [10] Trim, A.D., Braaten, H., Lie H. et. 2005, Experimental investigation of vortex-induced vibration of long marine risers [J]. *Journal of Fluids and Structures*, 21:335–361.
- [11] Huse E, Kleiven G, Nielsen F G, 1999, VIV-induced axial vibration on deep sea risers, *Proceedings of the Offshore Technology Conference*, Houston, Texas, OTC 10932.
- [12] Lie H, Kaasen H K, 2006, Modal analysis of measurements from a large-scale VIV model test of a riser in linearly sheared flow, *Journal of Fluid and Structures*, 22: 557-575.
- [13] XH Chen, Yu Ding, Jun Zhang et, 2006, Coupled dynamic analysis of a mini TLP: Comparison with measurements, *Ocean Engineering*, 33: 93-117.
- [14] J.K.VANDIVER. 1993, Dimensionless parameters important to the prediction of vortex-induced vibration of long, flexible cylinders in ocean currents [J]. *Journal of Fluids and Structures*. 7(5):423-455.
- [15] Zhang, LW, Chen WM, 2010, Study on the parameters for determining response types of long flexible riser undergoing VIV in deepwater, *China Offshore Oil and Gas*, 22(3):202-206.

ACKNOWLEDGMENTS

This work is supported by the National Natural Science Foundation of China (Grant No. 10772183) and The Intellectual Innovation Project of the Chinese Academy of Sciences (Grant No. KJCX2-YW-L07).

5. REFERENCE

- [1] Sarpkaya, T., 2004. A Critical review of the intrinsic nature of vortex-induced vibration. *Journal of Fluids and Structures Mechanics* 46, 389-447.
- [2] Grant R., Litton R., Finn, L., Maher J., Lambrakos K., Highly Compliant Rigid Risers: Field Test Benchmarking a Time Domain VIV Algorithm. OTC 11995, 2000.
- [3] Liao JC, Vandiver J.M. 2002, Vortex-induced vibration of slender structure in unsteady flow, Ph.D. dissertation, Massachusetts Institute of Technology
- [4] Chen WM, Zhang LW, Li M, 2009, Prediction of vortex-induced vibration of flexible riser using an improved wake-oscillator model. *Proceedings of the ASME 28th International Conference on Ocean, Offshore and Arctic Engineering OMAE2009*, May 2009, Honolulu, Hawaii.
- [5] Lyons G J, Patel MH. 1986, A prediction technique for vortex induced transverse response of marine risers and tethers. *Journal of Sound and Vibration*, 111 (3): 467-487.
- [6] Gei F, Hui L, Hong YS, 2007, Vortex-induced vibration of submarine floating tunnel undergoing shear flow. *Journal of the Graduate School of the Chinese Academy of Sciences*, 24(3):352-356. (in Chinese)
- [7] Bokaian A. 1994, Lock-in prediction of marine risers and tethers. *Journal of Sound and Vibration*, 175 (5): 607-623.
- [8] Khalak A.& Williamson C.H.K.. 1999, Motions, forces and mode transitions in vortex-induced vibrations at low mass-damping. *Journal of Fluids and Structures*, 13:813-851.